論　文

黒鉛に打ち込まれた水素同位体の脱離機構と再結合係数

渡　辺　国　昭 ・ 芦　田　　　完*

富山大学トリチウム科学センター
*富山大学放射性同位元素総合実験室
〒930 富山市五福3190番地

Desorption Mechanisms of Hydrogen Isotopes Implanted into Graphite and Recombination Factors

Kuniaki WATANABE　and *Kan ASHIDA

Tritium Research Center, Toyama University,
*Radio-isotope Labs., Toyama University,
Gofuku 3190, Toyama 930, Japan
(Received December 25, 1985)

Abstract

Kinetics and mechanisms were studied for the thermal release of hydrogen isotopes implanted into pyrolytic graphite. The kinetic measurements were carried out with mass analyzed thermal desorption spectroscopy. The desorption spectra consisted of three peaks, I, II, and III. The peak I obeyed the second order kinetics regarding the amount of trapped hydrogen isotope atoms. The recombination factors were evaluated and compared with those by other investigators. The recombination factors averaged over the sub-surface layer were determined as

$$k_r(H_2) = (13.0 \times 10^{-19})\exp(-44.0 \times 10^3/RT) \, [cm^4/sec \cdot molec]$$
$$k_r(D_2) = (7.18 \times 10^{-19})\exp(-44.0 \times 10^3/RT)$$
$$k_r(T_2) = (5.26 \times 10^{-19})\exp(-44.0 \times 10^3/RT)$$

The pseudo surface recombination factors were also determined as

$$k_s K^2(H_2) = (4.68 \times 10^{-3}) \exp(-44.0 \times 10^3/RT) \, [cm^2/sec \cdot molec]$$

$$k_s K^2(D_2) = (2.58 \times 10^{-3}) \exp(-44.0 \times 10^3/RT)$$

$$k_s K^2(T_2) = (1.89 \times 10^{-3}) \exp(-44.0 \times 10^3/RT)$$

It was concluded that the rate determining step for desorption forming the peak I was the surface recombination reaction of hydrogen isotope atoms trapped on the normal graphite lattice of the basal plane.

1 Introduction

Great attention has been paid to low-Z materials from the viewpoint of the application of these materials to the first wall for controlled thermonuclear fusion devices. Among those, graphite and/or carbon is considered to be the primary candidate materials[1] because of its low-Z, refractory nature, and ease in fabrication. However, there is a lack of systematic understanding of the wall processes such as wall bombardment, trapping and release by/of the particles escaping from the plasma[1]. From this viewpoint, we have studied trapping states and thermal release of hydrogen isotopes implanted into pyrolytic graphite by means of XPS-SIMS, mass analyzed thermal desorption spectroscopy, and Raman spectroscopy[2-11]. We have found that hydrogen isotopes are trapped in the graphite, at least, in two distinct states[5] and they are desorbed from the graphite in three different kinetics, making three desorption peaks in the thermal desorption spectra[4,7]. In addition, there is a considerable kinetic isotope effect in the desorption processes[7,10].

In this paper, we will describe the mechanisms of desorption of hydrogen isotopes forming the peak I and the recombination factors of three hydrogen isotopes.

2 Experimental

The sample used was a pyrolytic graphite (PG-A) purchased from Nihon Carbon Co. The sample size was 0.3 × 10 × 20mm. It was attached by screws to a sample holder made of stainless steel. The sample temperature was measured with a Pt/Pt-Rh(13%) thermocouple spot-welded to the Ta-sheet attached to the sample.

Hydrogen and deuterium gas were purchased from Showa Denko Co., being guaranteed as 99.999%(H$_2$) and 99.98%(D$_2$). Tritium gas in a glass ampoule (5 Ci) was purchased from New England Nuclear Co. According to mass spectroscopic analysis, the tritium gas contained such impurities as HT($\cong$30%), CH$_3$T($<$0.01%), HDO($<$0.02%), HTO($<$0.01%) and DTO($<$0.05%). These gases were used without further

purification.

An UHV system installed with XPS-SIMS optics was used for implantation and subsequent thermal desorption measurements for the non-radioactive isotopes. Another UHV apparatus was used for tritium implantation and desorption measurements.

After the implantation of hydrogen isotope ions, using conventional ion gun, into the sample at room temperature, the sample was heated to 950℃ to observe the thermal desorption spectra of H_2, D_2 or T_2. The details of the apparatuses and procedures have been described elsewhere[2,3,7].

3 Results

The thermal desorption spectra of hydrogen isotopes observed after the implantation gradually changed with repeating implantation-desorption cycles, coming steady and reproducible after the total implantation fluence exceeded 1×10^{19} ions/cm². This is a result of the modification of graphite surface due to accumulation of radiation damage[7,9]. The thermal desorption spectra for D_2 from the modified graphite surface are shown in Fig. 1. Those spectra were observed for the graphite implanted with the
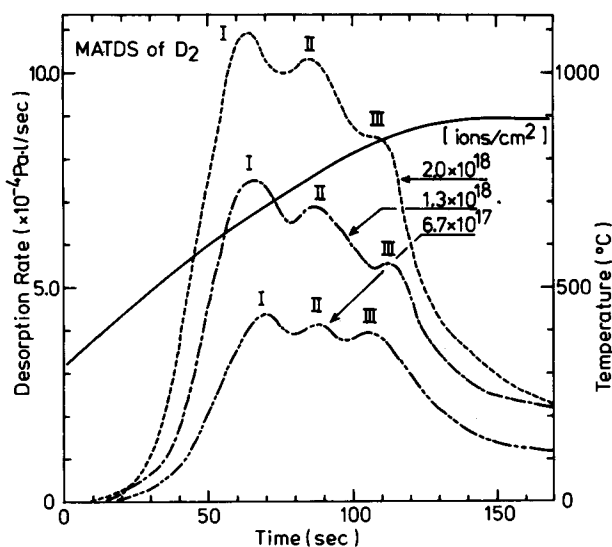

Fig. 1. Mass analyzed thermal desorption spectra of D_2 observed after deuterium ion implantation into graphite at room temperature.

deuterium ions of $6.7 \sim 20 \times 10^{17}$ ions/cm² with a temperature ramp of 5℃/min at about 770℃. Three desorption peaks appeared in each of the spectra, being denoted the

43

as I, II, and III as seen in the figure. The first peak appeared about 700℃ moved to the lower temperature side with increasing amount of the implantation. Namely, the increase in the ion fluence gave rise to the increase in the desorption amount and the peak shift toward the lower temperature side. Similar desorption spectra and peak shift were observed for the desorption of H_2[7] and T_2[10]. It was also observed that the peak temperature was a function of the temperature ramp.

On analogy of the "n"th order reaction in the conventional thermal desorption spectroscopy, the peak temperature, T_p, is considered to depend on the activation energy, E_d, frequency factor, ν_d, temperature ramp, β, and the concentration of hydrogen or its isotopes in the graphite, σ, as[12]

$$(E_d/RT_p^2) = (n\nu_d\sigma^{n-1}/\beta)\exp(-E_d/RT_p) \tag{1}$$

or rearranging as

$$\ln(T_p^2/\beta) = (E_d/RT_p) + \ln(E_d/nR\nu_d) - (n-1)\ln(\sigma) \tag{2}$$

Eq. (2) indicates that the plot of $\ln(T_p^2/\beta)$ against $(1/T)$ gives a straight line when
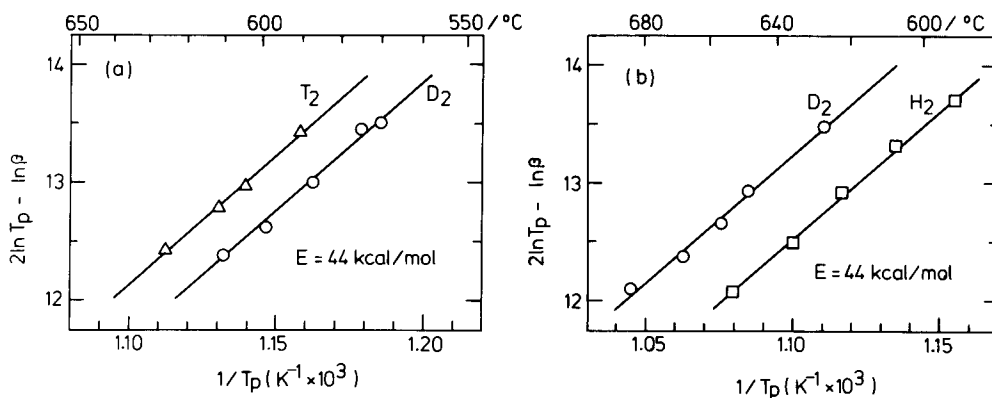

Fig. 2. (a) Plots of $\ln(T_p^2/\beta)$ vs $(1/T)$ for the desorption peak I for H_2 and D_2 observed with the XPS-SIMS system.
(b) Plots of $\ln(T_p^2/\beta)$ vs $(1/T)$ for the desorption peak I for D_2 and T_2 observed with the UHV system designed for tritium experiments.

the hydrogen concentration, σ, is kept constant in the experimental runs. Figure 2 shows examples of the plots for H_2, D_2 and T_2. A straight line was observed for each of the isotope, indicating that the above assumption is valid. From the slopes of these straight lines, the activation energies for desorption were evaluated as 44 kcal /mol for three isotopes : there was no isotope effect on the activation energy.

Another rearrangement of Eq. (1) gives

$$\ln(\beta E_d/RT_p^2) + (E_d/RT_p) = \ln(n\nu_d) + (n-1)\ln(\sigma) \qquad (3)$$

If E_d is known, the plots of "$\ln(\beta E_d/RT_p^2) + (E_d/RT_p)$" vs $\ln(\sigma)$ are possible, resulting in a straigkt line. The slope of it gives the reaction order. It has been determined as $n = 2$[7].

By use of this vaule, the frequency factor, ν_d, was determined from the intersect of the straight lines in Fig. 2 with the ordinate, because T_p and σ were measured directly from the desorption spectra, E_d and n were evaluated as the above, and β was a given parameter for the desorption spectra measurements. Following the procedures as the above, we obtained the rate constants for the peak I of H_2, D_2 and T_2 as

$$k_{ob}(H_2) = (6.0 \times 10^{-7}) \exp(-44.0 \times 10^3/RT) [1/\text{sec} \cdot \text{molec}] \qquad (4)$$

$$k_{ob}(D_2) = (3.0 \times 10^{-7}) \exp(-44.0 \times 10^3/RT) \qquad (5)$$

$$k_{ob}(T_2) = (2.0 \times 10^{-7}) \exp(-44.0 \times 10^3/RT) \qquad (6)$$

4 Discussion

4-1 Desorption Mechanisms

The second order kinetics is considered to be a result of the rate determining step for the desorption being the surface rocombination reaction of trapped hydrogen isotope atoms, which is indicated as "S-H" below in the case of hydrogen

$$2 \; S-H \xrightarrow{\quad} 2 \; S \; + H_2(g) \qquad (7)$$

$$-(1/2)d[C_s]/dt = d[H_2]/dt = N(t) = k_s C_s^2 \qquad (8)$$

Then, the desorption rate, $N(t)$, is described by Eq. (8), where k_s and C_s are the surface recombination factor and concentration of hydrogen atoms on the surface, respectively. Similar equation is valid for D_2 and/or T_2. In this case, it is considered that the diffusion rate of hydrogen atoms is fast in comparison with the rate of recombination reaction. Namely, an equilibrium is considerd to be established between the surface and sub-surface layer where hydrogen isotopes are implanted. This process is described by Eq. (9). Then, the surface concentration of hydrogen is expressed by Eq. (10), where K is the equilibrium constant, and N_s and N_b are the densities of the trapping sites on the surface and in the sub-surface layer, respectively : C_b is the concentration of hydrogen atoms trapped in the sub-surface layer.

$$B-H + \quad S \quad \Longleftrightarrow \quad B \quad + S-H \qquad (9)$$
$$C_b \qquad (N_s-C_s) \qquad\qquad (N_b-C_b) \qquad C_s$$
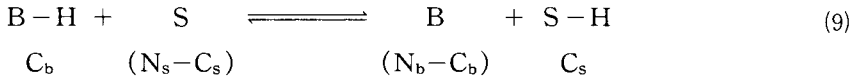
$$C_s = KN_sC_b/(N_b - C_b - KC_b) \tag{10}$$

By integrating thermal desorption spectrum, we can measure the amount of desorption : that is, the amount of trapped hydrogen atoms. The amount of trapped hydrogen responsible for making the peak I, n_T, is expressed by Eq. (11), where A and V are the surface area and volume of the sub-surface layer, respectively, in which hydrogen isotopes are implanted. Therefore, the surface concentration is written as Eq. (12).

$$n_T = C_sA + C_bV \tag{11}$$

$$C_s = KN_s(n_T - C_sA)/[VN_b - (1-K)(n_T - C_sA)] \tag{12}$$

In the case of the present study, the hydrogen isotope ions were implanted into the graphite with 5 keV. In this case, the range is considered to be about 6×10^{-6} cm. Namely, the majority of the implanted hydrogen isotopes are trapped in the sub-surface layer within the thickness of 6×10^{-6} cm. It means that the surface concentration is expressed by Eq. (13), because the relation $n_T \gg C_sA$ is valid in this case. In addition, if $VN_b \gg (1-K)n_T$, the relation is further simplified as Eq. (14). Then, the desorption rate is described by Eq. (15).

$$C_s = KN_s n_T / [VN_b - (1-K)n_T] \qquad (13)$$

$$= (KN_s/VN_b)n_T \qquad (14)$$

$$N(t) = k_s K^2 (N_s/VN_b)^2 n_T^2 \qquad (15)$$

$$N(t)_{ob} = k_{ob} n_T^2 \qquad (16)$$

This is exactly the same formula as the observed one, Eq. (15). Therefore, we conclude that the rate determining step for the desorption forming peak I is the surface recombination reaction of trapped hydrogen isotope atoms.

4-2　Recombination Factors

Comparing Eqs. (15) and (16), we obtain the following relation as

$$k_{ob} = k_s K^2 (N_s/N_b)^2 (A/V^2) \qquad (17)$$

The recombination factor has been conventionally defined as[13]

$$N(t) = k_r C^2 \qquad (18)$$

$N(t)$: desorption rate [molec/ $cm^2 \cdot sec$]

C 　 : hydrogen concentration in the sub-surface layer [atoms/cm^3]

k_r 　 : recombination factor [cm^4/ sec $\cdot$ molec]

where the surface roughness factor is assumed to be unity. It is mentioned here that the recombination factor thus defined is averaged over the sub-surface layer where hydrogen ions are implanted. Comparing this equation with Eq. (15), we obtain

$$k_r = k_s K^2 (N_s/N_b)^2 \qquad (19)$$

Substitution of this equation into Eq. (17) leads to

$$k_r = k_{ob}(V^2/A) \qquad (20)$$

Namely, the recombination factor is (V^2/A) times of the observed rate costant. In the present study, the beam of the implanting ions was 3mm in diameter : hence, the implanting area was $A = 0.071$ cm^2. The thickness of the sub-surface layer where hydrogen isotope ions were implanted is evaluated as 5.8×10^{-6} cm from the interpolation of Wampler's data[14] for D_2^+ ions of 5 keV. In addition, the ratio of the range among three hydrogen isotopes is evaluated as $R_H : R_D : R_T = 1 : 1.05 : 1.10$ from Schiøtt approximation[15]. Then, the volume of the sub-surface layer are $V(H) = 39.2 \times 10^{-8}$, $V(D) = 41.2 \times 10^{-8}$ and $V(T) = 43.2 \times 10^{-8} cm^3$. By use of these values (A and V),

and Eqs. (4), (5), (6) and (20), the recombination factors averaged over the sub-surface layer of the modified graphite for three hydrogen isotopes are determined as
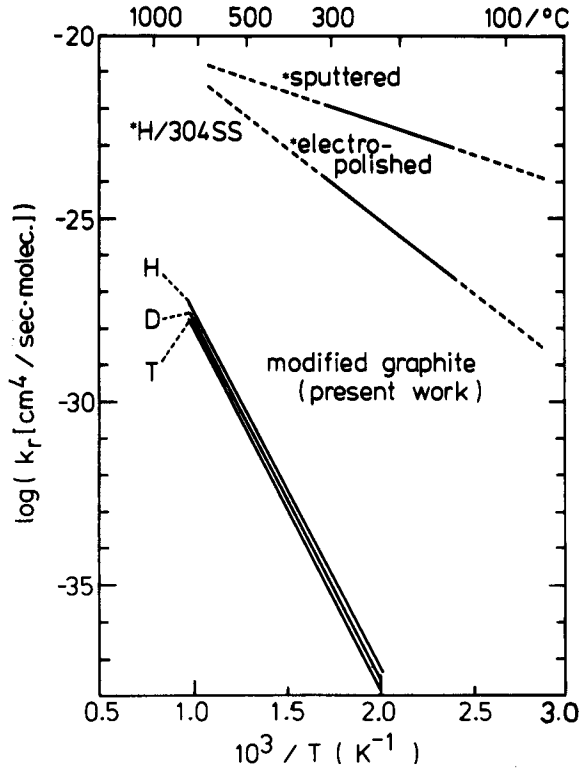

Fig. 3. Comparison of recombination factor, k_r, for graphite with that for stainless steel.
 * The data for stainless steel are taken from ref. [14]

$$k_r(H_2) = (13.0 \times 10^{-19})\exp(-44.0 \times 10^3/RT) [cm^4/sec \cdot molec] \qquad (21)$$

$$k_r(D_2) = (7.18 \times 10^{-19})\exp(-44.0 \times 10^3/RT) \qquad (22)$$

$$k_r(T_2) = (5.26 \times 10^{-19})\exp(-44.0 \times 10^3/RT) \qquad (23)$$

The recombination factors evaluated above are plotted in Fig. 3, where those for stainless steel are quoted from Langley[13] for the sake of comparison. It is seen in the figure that the recombination factors for the graphite are about five order of magnitude smaller than those for the stainless steel even at 1000℃.

The surface recombination rate of tritium estimated from the above factor is only 1×10^{14} molec/sec·cm^2 at 500℃ even at saturation concentration (c. a. 7×10^{22} atoms /cm^3) in graphite. The desorption rates of hydrogen isotopes forming the peak II and III should be far smaller than the above value. This indicates that the thermal release plays only a minor role for tritium recycling in the graphite first wall, especially at low temperature region : other mechanisms such as ion induced desorption will predominate

48

in the recycling of tritium in the graphite first wall.

The surface recombination factor, k_s, can not be evaluated from the observed rate constants, because the equilibrium constant, K, is unknown. We define here the pseudo surface recombination factor, $k_s K^2$. From Eq. (17), this is described as

$$k_s K^2 = (N_b/N_s)^2 (V^2/A) k_{ob}$$
$$= (N_b/N_s)^2 (V^2/A) \nu_d \exp(-E_d/RT) \qquad (24)$$

In this equation, the volume (V) and area (A) have been evaluated as the above. The trapping site densities, N_s and N_b, are calculated as follows. The atomic densities of carbon in graphite are $2.2 \times 10^{15}/cm^2$ on the surface and $1.1 \times 10^{23}/cm^3$ in the bulk. The saturation concentration of hydrogen atoms in graphite has been determined as $[H]/[C] \cong 0.5$[13,16,17]. Thus, the trapping site densities are $N_s = 1.1 \times 10^{15}/cm^2$ and $N_b = 6.6 \times 10^{22}/cm^3$. By use of these values, the pseudo surface recombination fac-tors are evaluated as

$$k_s K^2(H_2) = (4.68 \times 10^{-3}) \exp(-44.0 \times 10^3/RT) [cm^2/sec \cdot molec] \qquad (25)$$
$$k_s K^2(D_2) = (2.58 \times 10^{-3}) \exp(-44.0 \times 10^3/RT) \qquad (26)$$
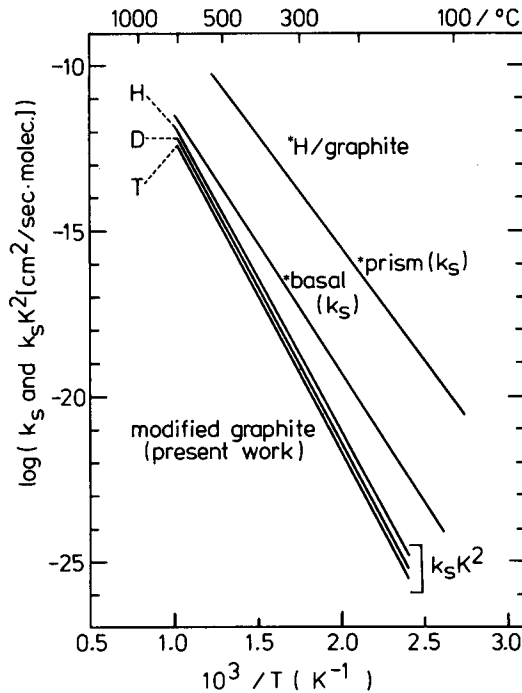$$k_s K^2(T_2) = (1.89 \times 10^{-3}) \exp(-44.0 \times 10^3/RT) \qquad (27)$$

Fig. 4. Comparison of the pseudo surface recombination factor, $k_s K^2$, evaluated from the present data with the surface recombination factor, k_s, for graphite.
  * The data for k_s are taken from ref. [18]

In Fig. 4, they are compared with the surface recombination factors, k_s, measured for a pyrolytic graphite by Balooch and Olander[18] as

$$k_s(H_2, \text{ basal plane}) = (2.6 \times 10^{-4}) \exp(-37.0 \times 10^3/RT) \ [\text{cm}^2/\text{sec} \cdot \text{moloc}]$$

$$k_s(H_2, \text{ prism plane}) = (2.1 \times 10^{-2}) \exp(-31.8 \times 10^3/RT)$$

The present results for H_2 are fairly near to Balooch's data on the basal plane, whereas they deviate considerably from those on prism plane. This is plausible from the point of view that the peak I has been attributed to the desorption of hydrogen isotope atoms trapped on the normal graphite lattice of basal plane[5,7]. The small deviation between the present results and Balooch's ones for the basal plane is considered to be due to that the former contains the equilibrium constant, K.

The surface recombination factor and equilibrium constant are functions of temperature as

$$k_s = \nu_s \exp(-E_s/RT) \tag{28}$$

$$K = \exp(\Delta S/R) \exp(-\Delta H/RT) \tag{29}$$

where E_s and ν_s are the activation energy and frequency factor for the surface recombination reaction, respectively. ΔH is the difference between the trapping energy (enthalpy) on the surface and that in the sub-surface layer, and ΔS the difference between the entropy of the trapped state of hydrogen atoms on the surface and that in the subsurface layer. Then, the temperature dependence of the pseudo surface recombination factor is described as

$$k_s K^2 = \nu_s \exp(2\Delta S/R) \exp[-(E_s + 2\Delta H)/RT] \tag{30}$$

Therefore, the activation energy and frequency factor in the pseudo surface recombination factor differ from those in the true surface recombination factor. From the difference in the frequency factors between the present results and Balooch's ones (basal plane), it is seen that $\Delta S > 0$, as expected : that is, the entropy of the trapped state on the surface is greater than that in the sub-surface layer.

5 Conclusions

In the present paper, we have analyzed the desorption of hydrogen isotopes forming the peak I in the desorption spectra for graphite. It is concluded that the rate determining step for the desorption is not the diffusion process, but the second

order surface recombination reaction.

The recombination factor of hydrogen isotopes averaged over the sub-surface layer where hydrogen ions are implanted are evaluated and compared with those for stainless steel. The results indicate that the recombination factor of hydrogen isotopes forming the peak I for the modified graphite are far smaller than those on stainless steel. The desorption rates of hydrogen isotopes making the peak II and III are much smaller than that of the peak I. An estimation suggests that the thermal release is not important on the recycling of tritium in graphite first wall especially at low temperature region.

The pseudo surface recombination factors of hydrogen isotopes are evaluated and compared with the surface recombination factors measured for graphite by other investigators. The comparison confirms the previous conclusion that the peak I appearing the desorption spectra is caused by the hydrogen isotope atoms trapped on the normal graphite lattice in the basal plane.

Acknowledgements

References

1) US-Japan Workshop Q-52 : "Plasma-Wall Interaction Data Needs Critical to a Burning Core Experiment", June 24-28, 1985, Sandia National Labs. (Livermore), USA.

2) K. Ashida, K. Ichimura, M. Matsuyama, H. Miyake and K. Watanabe, Ann. Rept. Tritium Res. Centr. Toyama Univ., **1** (1981) 15.

3) K. Ashida, K. Ichimura, M. Matsuyama, H. Miyake and K. Watanabe, J. Nucl. Mater., **111/112** (1982) 679.

4) K. Ashida, K. Ichimura and K. Watanabe, J. Vac. Soc. Jpn., **26** (1983) 397.

5) K. Ashida, K. Ichimura and K. Watanabe, J. Vac. Sci. Technol., **A1** (1983) 1465.

6) M. Matsuyama, K. Ashida and K. Watanabe, Ann. Rept. Tritium Res. Centr. Toyama Univ., **3** (1983) 71.

7) K. Ashida, K. Ichimura, M. Matsuyama and K. Watanabe, J. Nucl. Mater., **128/129** (1984) 792.

8) K. Ashida, K. Kanamori, M. Matsuyama and K. Watanabe, idid., **136** (1985) 284.

9) K. Ashida, K. Kanamori, K. Ichimura, M. Matsuyama and K. Watanabe, ibid., **137** (1986) 288.

10) K. Ashida, K. Ichimura and K. Watanabe, J. Vac. Soc. Jpn., in press.

11) K. Ashida and K. Watanabe, in this Journal.

12) P. A. Redhead, Vacuum, **12** (1962) 203.

13) R. A. Langley, J. Nucl. Mater., **128/129** (1984) 622.

14) W. R. Wampler, D. K. Brice and C. W. Magee, ibid., **102** (1981) 304.

15) H. E. Schiøtt, Radiation Effects, **6** (1970) 107.

16) R. A. Langley, R. S. Blewer and J. Roth, J. Nucl. Mater., **76/77** (1978) 313.

17) J. Roth, B. M. W. Scherzer, R. S. Blewer, D. K. Brice, S. T. Picraux and W. R. Wampler, ibid., **93/94** (1980) 601.

18) M. Balooch and D. R. Olander, J. Chem. Phys., **63** (1975) 4772.